

Investigation of Holographic Beamforming via Dynamic Metasurface Antennas in QoS Guaranteed Power Efficient Networks

Askin Altinoklu, and Leila Musavian

CSEE, University of Essex, UK

Emails: {askin.altinoklu, leila.musavian}@essex.ac.uk

Abstract—This work focuses on designing a power-efficient network for Dynamic Metasurface Antennas (DMAs)-aided multi-user multiple-input single output (MISO) antenna systems. The main objective is to minimize total transmitted power by the DMAs while ensuring a guaranteed signal-to-noise-and-interference ratio (SINR) for multiple users in downlink beamforming. Unlike conventional MISO systems, which have well-explored beamforming solutions, DMAs require specialized methods due to their unique physical constraints and wave-domain precoding capabilities. To achieve this, optimization algorithms relying on alternating optimization and semi-definite programming, are developed, including spherical-wave channel modelling of near-field communication. The dynamic reconfigurability and holography-based beamforming of metasurface arrays make DMAs promising candidates for power-efficient networks by reducing the need for power-hungry RF chains. On the other hand, the physical constraints on DMA weights and wave-domain precoding of multiple DMA elements through reduced number of RF suppliers can limit the degrees of freedom (DoF) in beamforming optimizations compared to conventional fully digital (FD) architectures. This paper investigates the optimization of downlink beamforming in DMA-aided networks, focusing on power efficiency and addressing these challenges.

I. INTRODUCTION

As the transition from 5G to 6G for mobile communication and internet of things networks is now rapidly progressing, key performance indicators (KPIs) and requirements for the communication standards of 6G networks became more apparent. It is well anticipated that the demand for data rate related KPIs such as the user experienced data rate and peak data rate will be among major concerns of 6G, as it was for 5G [1]. On the other hand, limitations on the overall power consumption of the future communication networks will be a significant concern under the paradigm shift toward green communications [2].

Considering that the number of devices involved in communication networks with various Quality of Services (QoS) constraints will be increased dramatically, and the typical data rates of future applications will be much higher than those of today, usage of distributed antenna apertures together with multiple-input multiple output (MIMO) and/or multiple-input single output (MISO) transmission will be inevitable for the future communication networks. On the other hand, with the effect of newly emerging technologies, distributed antenna arrays used within traditional MIMO/MISO systems are at the edge of transition from static predesigned intrinsic elements

to dynamically reconfigurable array elements such as metasurfaces [3]. The dynamic reconfigurability of metasurfaces, achieved through their physical properties such as permittivity and permeability, provides flexibility on the control and manipulation of electromagnetic (EM) waves that interact with them. Leveraging this characteristic, several distinct types of metasurface arrays have been developed in various applications of MIMO and MISO systems, whether as transmitter, receiver or within the wireless channel. Particularly, Dynamic Metasurface Antennas (DMAs) are shown to be as effective solution for downlink and uplink beamforming problems in MIMO and MISO systems [3]. Taking the leverage of wave-domain precoding, DMAs require less number of RF chains than the conventional MIMO and/or MISO architectures such as an FD architecture and do not need any additional analog circuitry such as phase shifters as in hybrid architectures. These features make DMAs a remarkable candidate for the low power communication networks. Recent studies based on DMAs show the effectiveness of beamforming in multiuser MISO downlink systems for information rate optimization problems [4], [5], [6].

On the other hand, the physical constraints on DMA weights, such as Lorentzian-constrained polarizability, and wave-domain precoding of DMA elements can limit the Degree-of-Freedom (DoF) of DMA when compared to conventional FD architectures. Although increasing the number of DMA elements, with its ability to decrease element spacing below $\lambda/2$ limit of conventional arrays, can alleviate these limitations, the impact on beamforming is not well-understood yet. This work aims to investigate these effects on DMA-aided power-efficient networks through optimal beamforming under signal-to-noise-and-interference ratio (SINR) constraints. Our main contributions are as follows: i) we derive the optimal multiuser holographic beamforming solution to satisfy SINR requirements of all users while minimizing transmitted power in MISO networks, ii) we propose a holographic beamforming method based on semi-definite relaxation, solvable using convex optimization tools, and demonstrate its robustness across various scenarios, and iii) we perform comprehensive Monte-Carlo simulations with randomly located users for different scenarios, to highlight the impact of Lorentzian-constrained polarizability and reduced number of RF chains on the optimal beamforming and the transmitted power in comparison

to the unconstrained generic optimization problems, and iv) we analyze these effects across varying parameters, such as user position, number of users, and antenna element spacing, in comparison to the results of FD architecture, providing valuable insights for optimal DMA parameter selection.

Notations:

A matrix is denoted by the boldface capital \mathbf{W} with $\text{rank}(\mathbf{W})$, $\text{Tr}(\mathbf{W})$, \mathbf{W}^T , \mathbf{W}^H , and $\text{Vec}(\mathbf{W})$ representing its rank, trace, transpose, Hermitian conjugate, and vectorization, respectively. A vector is denoted by the boldface lower-case \mathbf{w} , with $\|\mathbf{w}\|$, \mathbf{w}^T , and \mathbf{w}^H indicating its Euclidean norm, transpose, and Hermitian conjugate, respectively. The unit vector in the direction of \mathbf{w} is denoted by $\hat{\mathbf{w}}$, while the scalar is represented by w , and $|w|$ is its absolute value. The Kronecker product is indicated by \otimes .

II. SYSTEM MODEL & PROBLEM FORMULATION

We consider a multi-user downlink MISO system, where the base station (BS) is equipped with either FD-aided or DMA-aided beamforming architectures. In this system, the BS serves K users, each equipped with a single antenna and requesting a certain level of SINR, in a generic Line-of-Sight (LoS) channel model that covers both far-field and near-field users. Moreover, perfect knowledge of the channel is assumed.

A. Channel and Path-Loss Modeling

In order to obtain channel modeling, we consider modeling with a uniform planar array (UPA) consisting of N_r and N_c subwavelength elements in the vertical and horizontal directions, respectively. This yields a total of $N = N_r N_c$ radiating subwavelength elements. The radiation pattern $G_e(\psi)$ of individual elements above a conducting plate is well-approximated with ([7]):

$$G_e(\psi) = \begin{cases} 2(g+1)\cos^g(\psi), & 0 \leq \psi \leq \pi/2 \\ 0, & \pi/2 < \psi \leq \pi \end{cases} \quad (1)$$

where ψ is the angle measured from the Boresight of the array, g is the measure of antenna gain. In our problem, we consider subwavelength elements as dipoles, i.e., $g = 2$.

As the elements with $G_e(\psi)$ radiate over the free-space, propagation of electromagnetic waves towards user position (\mathbf{r}_k) from the (i,l) -th element of the UPA ($\mathbf{r}_{i,l}$) can be expressed for the channel as follows:

$$\gamma_k(i,l) = \sqrt{G_e(\psi)} \frac{\lambda}{4\pi\|\mathbf{r}_k - \mathbf{r}_{i,l}\|} e^{-j\beta_0\|\mathbf{r}_k - \mathbf{r}_{i,l}\|}, \quad (2)$$

where λ , and β_0 are the free-space wavelength and wavenumber, respectively. The entries $\gamma_k(i,l)$ are the elements of the channel vector $\boldsymbol{\gamma}_k \in \mathbb{C}^{N \times 1}$, i.e., $\boldsymbol{\gamma}_k \triangleq [\gamma_k(1,1), \gamma_k(1,2), \dots, \gamma_k(N_r, N_c)]^H$.

B. FD Architecture

In the FD-based architecture, data streams s_k for $k = 1, 2, \dots, K$ are transmitted via a UPA consisting of N antennas. Each antenna element is excited by a separate RF chain, and the desired beams are created using digital beamforming vectors $\mathbf{w}_m \in \mathbb{C}^{N \times 1}$ for all $m = 1, 2, \dots, M$, where M is the number of beam-forming vectors. Accordingly, the transmitted signal can be written as:

$$\mathbf{x}^{\text{FD}} = \sum_{m=1}^M \mathbf{x}_m^{\text{FD}} = \sum_{m=1}^M \mathbf{w}_m s_m. \quad (3)$$

By inserting (3) into (2), the signal received at User k can be defined as

$$y_k = \boldsymbol{\gamma}_k^H \sum_{m=1}^M \mathbf{w}_m s_m + n_k, \quad (4)$$

where $n_k \sim \mathcal{CN}(0, \sigma^2)$ is the white Gaussian noise for the k -th channel, and $\mathbb{E}[s_m^2] = 1$ for all $m = 1, 2, \dots, M$.

C. DMA Architecture

The DMA-based architecture comprises of N_r microstrips each containing N_c metasurface-based intrinsic elements, yielding $N \triangleq N_c N_r$ of total elements. The metasurface elements are excited by guided (reference) waves propagating through each associated microstrip. The sampling of these reference waves at the antenna locations can be represented by the matrix $\mathbf{H} \in \mathbb{C}^{N \times N}$. Each microstrip is connected to the digital beamformer through a single RF chain and the complex amplitudes of the reference wave for each microstrip are controlled by digital beamforming vectors $\mathbf{w}_m \in \mathbb{C}^{N_r \times 1}$ for all $m = 1, 2, \dots, M$, where $M = \min(K, N_r)$. The radiated pattern of individual elements is further adjusted with their corresponding dynamically configurable weights ($\mathbf{Q} \in \mathbb{C}^{N \times N_c}$). Hence, the transmitted signal from DMA aperture and the channel input can be written as

$$\mathbf{x}^{\text{DMA}} = \sum_{m=1}^M \mathbf{x}_m^{\text{DMA}} = \sum_{m=1}^M \mathbf{H} \mathbf{Q} \mathbf{w}_m s_m. \quad (5)$$

In (5), assuming that the individual elements are excited only by the microstrip that are on, the matrix \mathbf{H} takes the form of a diagonal matrix as defined with $\mathbf{H}_{(i-1)N_c+l, (i-1)N_c+l} = e^{-d_{i,l}(\alpha_i + j\beta_i)}$, where $d_{i,l}$ represents the position of the l -th element along the i -th microstrip, while α_i and β_i are the attenuation, and propagation constants for the i -th microstrip, respectively. The matrix \mathbf{Q} includes the inter-connectivity of the individual elements to the excitation ports, with their frequency-dependent response to the external excitation. This response can be well-defined by the Lorentzian resonance response, i.e.,

$$\mathbf{Q} = \left\{ q = \frac{j + e^{j\Phi}}{2} : \Phi \in [0, 2\pi] \right\}. \quad (6)$$

Assuming no mutual-coupling between adjacent microstrips, the matrix \mathbf{Q} takes a block-diagonal form as described with

$$\mathbf{Q}_{(i-1)N_c+l, n} = \begin{cases} q_{i,l} \in \mathbf{Q} & \text{if } i = n \\ 0 & \text{if } i \neq n. \end{cases} \quad (7)$$

Finally, by inserting the antenna aperture distributions from (5) into the channel model given in (2), the signal received at User k can be defined as

$$y_k^{\text{DMA}} = \gamma_k^H \sum_{m=1}^M \mathbf{H}\mathbf{Q}\mathbf{w}_m s_m + n_k. \quad (8)$$

D. General Problem Formulation

Following the derivations of transmitted and received signals \mathbf{x}_k , \mathbf{y}_k for each user, SINR can be expressed by

$$\text{SINR}_k = \frac{|\gamma_k^H \mathbf{x}_k|^2}{\sum_{\substack{m=1 \\ m \neq k}}^M |\gamma_k^H \mathbf{x}_m|^2 + \sigma_k^2}, \quad (9)$$

where σ_k^2 is the noise power for the k -th channel. The information rate for User k can then be calculated as $R_k = \log_2(1 + \text{SINR}_k)$.

Given that optimization aim of the downlink beamforming problem is to minimize the total transmit power under the constraints of given sets of SINR for different users, the problem can be expressed as

$$\begin{aligned} & \underset{\mathbf{x}_m, \forall m}{\text{minimize}} && \sum_{m=1}^M \|\mathbf{x}_m\|^2 \\ & \text{s.t.} && \frac{|\gamma_k^H \mathbf{x}_k|^2}{\sum_{\substack{m=1 \\ m \neq k}}^M |\gamma_k^H \mathbf{x}_m|^2 + \sigma_k^2} \geq \delta_k, \quad \forall k \in K, \end{aligned} \quad (10)$$

where $\delta_1, \dots, \delta_k$ represent the SINR thresholds that must be guaranteed for each user. For convexity it can be said that, (10) is not convex due to the definition of SINR in the constraints. However, it is shown that it can be reformulated in the form of convex semidefinite program (SDP) [8] as

$$\underset{\mathbf{X}_m}{\text{minimize}} \quad \sum_{m=1}^M \text{Tr}(\mathbf{X}_m) \quad (11a)$$

$$\text{s.t.} \quad \text{Tr}(\mathbf{\Gamma}_k \mathbf{X}_k) - \delta_k \sum_{\substack{m=1 \\ m \neq k}}^M \text{Tr}(\mathbf{\Gamma}_k \mathbf{X}_m) - \delta_k \sigma_k^2 \geq 0, \quad \forall k \in K, \quad (11b)$$

$$\mathbf{X}_m \succeq 0 \quad \forall m \in M, \quad (11c)$$

where $\mathbf{X}_m = \mathbf{x}_m \mathbf{x}_m^H$, $\mathbf{\Gamma}_k = \gamma_k \gamma_k^H$, and $\mathbf{X}_m \succeq 0$ implies that \mathbf{X}_m is positive semidefinite. Problem (11) is the dual of original problem (10) as long as the optimal solution \mathbf{X}_m is rank-1, i.e., SDP relaxation (SDR) is satisfied. For (11), it is known that there exists at least one optimal solution where all \mathbf{X}_m have rank one. Therefore, global optimal solutions for original problem (10) can be obtained by solving (11) using convex optimization tools such as CVX [9] and performing eigenvalue decomposition (EVD) for \mathbf{X}_m for all m .

For FD-based architecture, the problem in (10) is solved with $\mathbf{x}_m = \mathbf{x}_m^{\text{FD}}$, and $\mathbf{X}_m = \mathbf{W}_m$, where $\mathbf{W}_m = \mathbf{w}_m \mathbf{w}_m^H$. Typically, the element spacing for FD-based architecture is limited by a lower bound of $\lambda/2$, where λ represents the free-space wavelength. However, DMA-based architectures allow for denser element placement, enabling spacing smaller than

this lower bound of FD-based architectures. For comparison purposes, we also solve problem (11) for the case where $d < \lambda/2$, which we refer to as Optimization Problem 1(OP1). In OP1, only the digital precoding vector ($\mathbf{w}_m \in \mathbb{C}^{N \times 1}$) is involved in the optimization, where the number of optimization parameters equal to the number of array elements and each parameter can be freely chosen in the complex domain. This enables OP1 to represent a physically non-realizable boundary for DMA optimizations, serving as a benchmark with unconstrained DMA weights and the maximum number of degrees of freedom (DoF) in terms of optimization parameters.

III. PROPOSED BEAMFORMING OPTIMIZATION SOLUTION FOR DMA

For DMA-based architecture, the optimization problem in (10) can be revised with $\mathbf{x}_m^{\text{DMA}} = \mathbf{H}\mathbf{Q}\mathbf{w}_m$, which can be derived as

$$\underset{\mathbf{Q}, \mathbf{w}_m, \forall m}{\text{minimize}} \quad \sum_{m=1}^M \|\mathbf{H}\mathbf{Q}\mathbf{w}_m\|^2 \quad (12a)$$

$$\text{s.t.} \quad \frac{|\gamma_k^H \mathbf{H}\mathbf{Q}\mathbf{w}_k|^2}{\sum_{\substack{m=1 \\ m \neq k}}^M |\gamma_k^H \mathbf{H}\mathbf{Q}\mathbf{w}_m|^2 + \sigma^2} \geq \delta_k, \quad \forall k \in K, \quad (12b)$$

$$q_n \in \mathbb{Q}, \quad \forall n \in N. \quad (12c)$$

The optimization problem for the DMA-based architecture, as given in (12), differs from the one in (10). In the DMA-based optimization problem, the digital precoder vectors \mathbf{w}_m , and the DMA weights \mathbf{Q} are coupled to each other. Moreover, the amplitudes and phases of the individual elements q_n are dependent on each other, and the phases are limited to the range $[0, \pi]$. These differences make the problem challenging to obtain the optimal solution. The solution of problem (12) requires the joint design of the precoding vector and the DMA weights, where we divide the problem into two decoupled stages to perform optimization for each of the variables individually. Optimization of the digital precoder vectors (\mathbf{w}_m), and the DMA weights (\mathbf{Q}) are performed in an alternating manner based on the SDR formulations [5].

A. Optimizing the Digital Precoder

When \mathbf{Q} is fixed, (11a) can be rewritten to derive the total transmitted power $P_{\text{Tx}}^{\text{DMA}}$ as follows:

$$\begin{aligned} P_{\text{Tx}}^{\text{DMA}} &= \sum_{m=1}^M \text{Tr}(\mathbf{X}_m^{\text{DMA}}) = \sum_{m=1}^M \text{Tr}((\mathbf{H}\mathbf{Q}\mathbf{w}_m)(\mathbf{H}\mathbf{Q}\mathbf{w}_m)^H) \\ &= \sum_{m=1}^M \text{Tr}(\mathbf{Z}\mathbf{W}_m), \end{aligned} \quad (13)$$

where $\mathbf{Z} = (\mathbf{H}\mathbf{Q})^H \mathbf{H}\mathbf{Q}$. Moreover, the received power at User k due to the m -th beamforming vector of the DMA ($P_{\text{Rx},k,m}^{\text{DMA}}$) can be derived as a function of \mathbf{W}_m :

$$\begin{aligned} P_{\text{Rx},k,m}^{\text{DMA}} &= \text{Tr}(\gamma_k^H \mathbf{H}\mathbf{Q}\mathbf{w}_m \mathbf{w}_m^H (\gamma_k^H \mathbf{H}\mathbf{Q})^H) \\ &= \text{Tr}(\mathbf{P}_k \mathbf{W}_m), \end{aligned} \quad (14)$$

where $\mathbf{P}_k = \gamma_k^H \mathbf{H}\mathbf{Q}(\gamma_k^H \mathbf{H}\mathbf{Q})^H$. Then, combining (13) and

(14), optimization problem (12) can be reformulated in SDP relaxation form as

$$\begin{aligned} & \underset{\mathbf{W}_m}{\text{minimize}} && \sum_{m=1}^M \text{Tr}(\mathbf{Z}\mathbf{W}_m) \\ \text{s.t.} &&& \text{Tr}(\mathbf{P}_k \mathbf{W}_k) - \delta_k \sum_{\substack{m=1 \\ m \neq k}}^M \text{Tr}(\mathbf{P}_k \mathbf{W}_m) - \delta_k \sigma_k^2 \geq 0, \quad \forall k \in K, \\ &&& \mathbf{W}_m \succeq 0, \quad \forall m \in M. \end{aligned} \quad (15)$$

After solving the SDP problem defined in (15), the digital precoding vectors $\mathbf{w}_m \in \mathbb{C}^{N_r \times 1}$ can be obtained via eigenvalue decomposition (EVD) of the associated matrix \mathbf{W}_m and this solution is global optimum solution if \mathbf{W}_m is rank-1 (see e.g., [8], Sec. 18.4.2).

B. Optimizing the DMA Weights

When \mathbf{w}_m for $\forall m \in M$ is fixed, the formulations for the optimization of the DMA weights \mathbf{Q} can be derived by reformulating (12) in the form of an SDP relaxation, where the variable in the optimization problem is set to be \mathbf{Q} . Utilizing the identity $\mathbf{A}^T \mathbf{Q} \mathbf{b} = (\mathbf{b}^T \otimes \mathbf{A}^T) \text{Vec}(\mathbf{Q})$ [4], $\mathbf{x}_m^{\text{DMA}}$ can be rewritten as:

$$\mathbf{x}_m^{\text{DMA}} = \mathbf{H} \mathbf{Q} \mathbf{w}_m = (\mathbf{w}_m^T \otimes \mathbf{H}) \text{vec}(\mathbf{Q}). \quad (16)$$

Then, by defining $\mathbf{A}_m = (\mathbf{w}_m^T \otimes \mathbf{H})^H \in \mathbb{C}^{L \times N}$ and the vector $\mathbf{q} = \text{vec}(\mathbf{Q}) \in \mathbb{C}^{L \times 1}$, where $L = N_r^2 N_c$, the total transmitted power $P_{\text{Tx}}^{\text{DMA}}$ can be derived as follows:

$$P_{\text{Tx}}^{\text{DMA}} = \sum_{m=1}^M \text{Tr}(\mathbf{X}_m^{\text{DMA}}) = \sum_{m=1}^M \text{Tr}(\mathbf{A}_m^H \mathbf{q} \mathbf{q}^H \mathbf{A}_m). \quad (17)$$

By defining $\tilde{\mathbf{q}} \in \mathbb{C}^{N \times 1}$, obtained by removing all the zero elements from \mathbf{q} , and $\tilde{\mathbf{A}}_m \in \mathbb{C}^{N \times N}$, formed by removing the rows corresponding to the indices of the removed elements in \mathbf{q} , (17) can be rewritten as:

$$P_{\text{Tx}}^{\text{DMA}} = \sum_{m=1}^M \text{Tr}(\tilde{\mathbf{A}}_m^H \tilde{\mathbf{q}} \tilde{\mathbf{q}}^H \tilde{\mathbf{A}}_m) = \sum_{m=1}^M \text{Tr}(\tilde{\mathbf{B}}_m \tilde{\mathbf{Q}}), \quad (18)$$

where $\tilde{\mathbf{B}}_m = \tilde{\mathbf{A}}_m \tilde{\mathbf{A}}_m^H$ and $\tilde{\mathbf{Q}} = \tilde{\mathbf{q}} \tilde{\mathbf{q}}^H$.

Following the derivations for $P_{\text{Tx}}^{\text{DMA}}$, the received power at User k due to the m -th beamforming vector of the DMA $P_{\text{Rx},k,m}^{\text{DMA}}$ can be derived similarly. Given the fact that $\mathbf{a}^T \mathbf{Q} \mathbf{b} = (\mathbf{b}^T \otimes \mathbf{a}^T) \text{vec}(\mathbf{Q})$, $y_{k,m}^{\text{DMA}}$ given in (8) can be defined and reformulated as

$$y_{k,m}^{\text{DMA}} = (\mathbf{w}_m^T \otimes (\gamma_k^H \mathbf{H})) \text{vec}(\mathbf{Q}) = \mathbf{c}_{k,m}^H \mathbf{q}, \quad (19)$$

where $\mathbf{c}_{k,m} = (\mathbf{w}_m^T \otimes (\gamma_k^H \mathbf{H}))^H \in \mathbb{C}^{L \times 1}$. Furthermore, the modified vectors, obtained by removing zero elements as described above, can be defined as $\tilde{\mathbf{c}}_{k,m} \in \mathbb{C}^{N \times 1}$ and $\tilde{\mathbf{q}} \in \mathbb{C}^{N \times 1}$. Then, $P_{\text{Rx},k,m}^{\text{DMA}}$ can be further simplified as:

$$P_{\text{Rx},k,m}^{\text{DMA}} = \text{Tr}(\tilde{\mathbf{c}}_{k,m}^H \tilde{\mathbf{q}} (\tilde{\mathbf{c}}_{k,m}^H \tilde{\mathbf{q}})^H) = \text{Tr}(\tilde{\mathbf{C}}_{k,m} \tilde{\mathbf{Q}}), \quad (20)$$

where $\tilde{\mathbf{C}}_{k,m} = \tilde{\mathbf{c}}_{k,m} \tilde{\mathbf{c}}_{k,m}^H$.

Finally, combining (18) and (20) the optimization problem is formulated as

$$\begin{aligned} & \underset{\tilde{\mathbf{Q}}}{\text{minimize}} && \sum_{m=1}^M \text{Tr}(\tilde{\mathbf{B}}_m \tilde{\mathbf{Q}}) \\ \text{s.t.} &&& \text{Tr}(\tilde{\mathbf{C}}_{k,k} \tilde{\mathbf{Q}}) - \delta_k \sum_{\substack{m=1 \\ m \neq k}}^M \text{Tr}(\tilde{\mathbf{C}}_{k,m} \tilde{\mathbf{Q}}) - \delta_k \sigma_k^2 \geq 0, \quad \forall k \in K, \\ &&& \tilde{\mathbf{Q}} \succeq 0. \end{aligned} \quad (21)$$

Algorithm 1 Proposed algorithm for solving problem (12)

Initialize: $\mathbf{Q}^{(0)}$;

Solve (15) to calculate $\{\mathbf{W}^{(0)}\}_{m=1}^M$;

Update $\{\mathbf{w}^{(0)}\}_{m=1}^M$ and $P_{\text{Tx}}^{(0)}$ based on $\{\mathbf{W}^{(0)}\}_{m=1}^M$;

for $t = 1, \dots, T$ **do**

Solve (21) to calculate $\tilde{\mathbf{Q}}^* \in \mathbb{C}^{N \times N}$ based on $\{\mathbf{w}^{(t-1)}\}_{m=1}^M$;

Calculate $\tilde{\mathbf{q}}^* \in \mathbb{C}^{N \times 1}$ based on $\tilde{\mathbf{Q}}^* \in \mathbb{C}^{N \times N}$;

Calculate $\tilde{\mathbf{q}}$ with Lorentzian Mapping of $\tilde{\mathbf{q}}^* \in \mathbb{C}^{N \times 1}$;

Update $\mathbf{Q}^{(t)}$ for problem (12) based on $\tilde{\mathbf{q}}$ and (7);

Solve (15) to calculate $\{\mathbf{W}^{(t)}\}_{m=1}^M$ based on $\mathbf{Q}^{(t)}$;

Update $\{\mathbf{w}^{(t)}\}_{m=1}^M$ and $P_{\text{Tx}}^{(t)}$ based on $\{\mathbf{W}^{(t)}\}_{m=1}^M$;

end for

if $P_{\text{Tx}}^{(t)} \leq P_{\text{Tx}}^{(t-1)}$ **then**

$\{\mathbf{w}^{(f)}\}_{m=1}^M \leftarrow \{\mathbf{w}^{(t)}\}_{m=1}^M$; $\mathbf{Q}^{(f)} \leftarrow \mathbf{Q}^{(t)}$;

$P_{\text{Tx}}^{(f)} \leftarrow P_{\text{Tx}}^{(t)}$;

end if

Output: $\{\mathbf{w}^{(f)}\}_{m=1}^M$, $\mathbf{Q}^{(f)}$, $P_{\text{Tx}}^{(f)}$.

For given digital precoding vectors $\{\mathbf{w}_m^*\} \forall m \in M$, the solution of (21) yields the optimal matrix $\tilde{\mathbf{Q}}^* \in \mathbb{C}^{N \times N}$. The vector $\tilde{\mathbf{q}}^* \in \mathbb{C}^{N \times 1}$ can then be obtained via the EVD of $\tilde{\mathbf{Q}}^*$. The special case solution of problem (12) can be defined when the condition in (12c), i.e, $q_n \in \mathbb{Q}$ is relaxed to $q_n \in \mathbb{C}^{N \times 1}$. We refer to this scenario as "unrestricted weights" scenario, since the amplitudes and phases of the weights can be optimized freely within the complex domain ($\mathbb{C}^{N \times 1}$). However, when performing optimization with a DMA-based architecture using (12), the solution vector $\tilde{\mathbf{q}}^*$ must be mapped onto the Lorentzian circle described in (6). For this mapping, we use the method described in [6], specifically, the entry-wise projection that aims to find the nearest points on the Lorentzian circle, $\tilde{q}_n \in \tilde{\mathbf{q}}$, from the elements of the solution vector $\tilde{q}_n^* \in \tilde{\mathbf{q}}^*$. The problem (21) can be considered as a relaxation of the problem in (12) based on the Lorentzian constraints without mapping. This additional step of Lorentzian Mapping ensures that the optimized DMA weights adhere to the behavior described in (6). In this behavior, the amplitudes and phases of the DMA weights are constrained by the Lorentzian relation. According to this relation, the amplitude of the DMA weights for individual elements is determined by the corresponding phase shift of those elements, which is

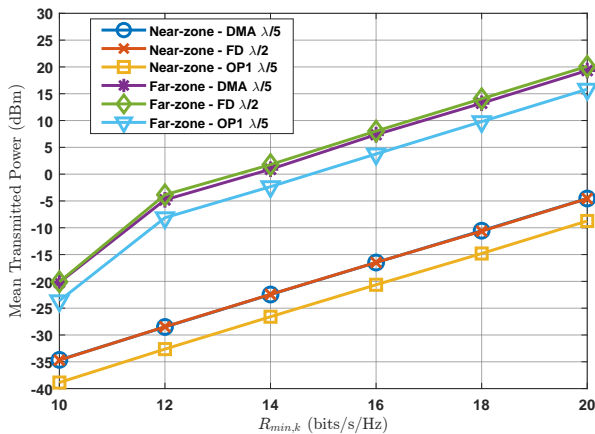


Fig. 1: Mean transmitted power versus minimum rate requirement at $K = 2$.

restricted to the range $[0, \pi]$. As a result, these constraints lead to a loss of performance. Finally, solving the individual problems (15) and (21) in an alternating way effectively leads to the convergence of the digital precoder vectors toward the optimal solution, while optimizing the DMA weights toward suboptimal solutions. This approach is encapsulated in the proposed algorithm, which is detailed in Algorithm 1.

IV. NUMERICAL RESULTS

In the numerical results, we consider the simulation setup that a uniform planar array is placed in the xy -plane, and the users are randomly distributed over 200 realizations within the half-circles with radius R lie in the xz -plane, covering both near-zone ($0.1d_F < R < 1d_F$) and far-zone regions ($1d_F < R < 5d_F$). Here, d_F is the Fraunhofer distance, i.e., $d_F \triangleq \frac{2D^2}{\lambda}$ for antenna aperture length of D and wavelength λ . Throughout the experimental study, the frequency is set to $f = 28$ GHz, and the aperture size is consistently fixed at $10 \text{ cm} \times 10 \text{ cm}$ for all structures. Optimizations are performed to guarantee the minimum achievable rate for each user ($R_{\min,k}$), which can be related to the SINR conditions in optimization problems by $\delta_k \triangleq (2^{R_{\min,k}} - 1)$, where $R_{\min,k}$ is the same for all k . The noise power is set to $\sigma_k^2 = -114$ dBm. For DMA, flat frequency characteristics are achieved by assuming the \mathbf{H} matrix is an identity matrix. For all structures, the separation between rows of the UPA is kept constant at $d_y = \lambda/2$, where $N_r = \lfloor 2D/\lambda \rfloor$. The separation between columns of the UPA, denoted by d_x , is varied for the case of DMA, while it is fixed at $d_x = \lambda/2$ for the FD-based architecture as a benchmark.

To demonstrate the robustness of the proposed optimization algorithm for DMA, we perform a performance analysis of the mean transmit power as a function of the minimum rate constraint $R_{\min,k}$ for $K = 2$ user realizations in different zones (Zone 1: near-zone, Zone 2: far-zone), as given in Fig. 1. Three optimization scenarios are considered: (1) DMA with $d_x = \lambda/5$, (2) FD with $d_x = \lambda/2$, and (3) OP1 (Problem (11)) with $d_x = \lambda/5$, highlighting the optimal boundary for DMA

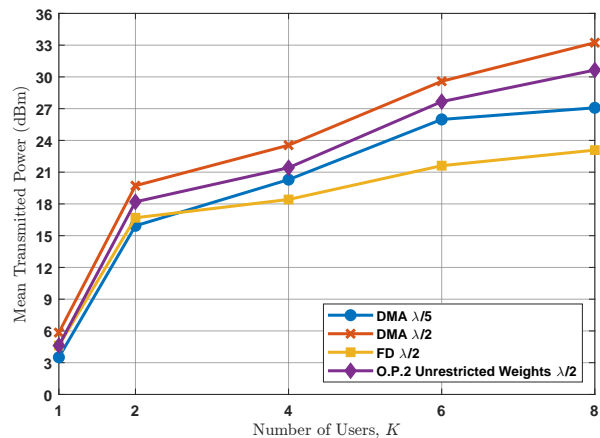


Fig. 2: Mean transmitted power versus number of users (K) at $R_{\min,k} = 20$ bps/Hz for $\forall k$.

in terms of DoF. As expected, the mean transmitted power increases linearly as the minimum rate requirement increases. While DMA with $d_x = \lambda/5$ and FD with $d_x = \lambda/2$ performs very similar, DMA requires, on average, 4.2 dBm and 3.3 dBm higher transmit power compared to OP1 with $d_x = \lambda/5$ in the near-zone and far-zone, respectively. This constant difference can be related to the performance gap caused by the reduced number of DoF for DMA.

Next, we perform further analysis, as illustrated in Fig. 2, examining the mean transmit power versus the number of users, with a minimum rate constraint $R_{\min,k} = 20$ bits/s/Hz for all users. In this analysis, 200 realizations are performed for a region covering both the near-zone and far-zone users. Optimization scenarios, i.e., DMA, FD, and OP2- Unrestricted Weights (UW) (see Section III.B) are considered, all with the same antenna spacing $d_x = \lambda/2$ to ensure the same number of antennas across all structures. Additionally, DMA with $d_x = \lambda/5$ is included for comparison purposes. It has been observed that the performance gap between DMA and FD with the same antenna spacing $d_x = \lambda/2$, gradually increases as number of users increases. Numerically, the difference in mean transmit power demands grows from 2.3 dB for $K = 1$ to 10.2 dB for $K = 8$. Meanwhile, DMA with $d_x = \lambda/5 \forall k$, offers better performance in terms of mean transmit power for $K = 1, 2$ than FD, while FD with $d_x = \lambda/2$ outperforms it for a higher number of users ($K > 2$). This yields that DMA requires denser array placement than $d_x = \lambda/5$ to achieve the same performance as FD under these conditions for ($K > 2$).

To examine the effect of DoF for both Lorentzian mapping and number of optimization variables, we can further compare the results of DMA and FD with OP2-UW under the same antenna spacing at $d_x = \lambda/2$. The comparison between OP2-UW and DMA highlights the impact of restrictions on DMA weights with Lorentzian mapping. Specifically, the performance gap is approximately 1.1 dBm for $K = 1$, increasing to 2.6 dBm as K reaches to 8. On the other hand, comparison of FD and OP2-UW can be interpreted in terms of impact of number of optimization variables on achievable transmit

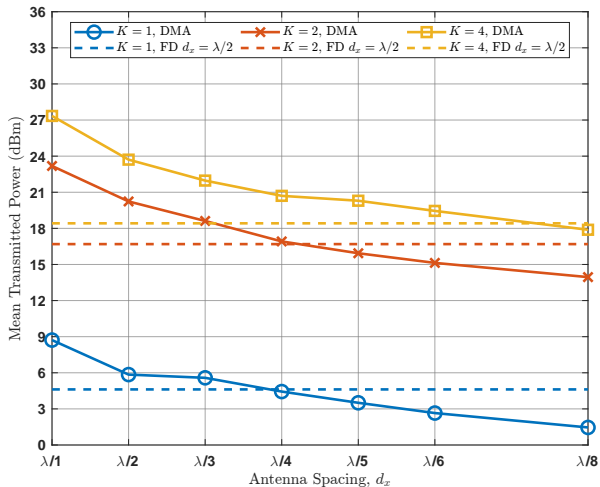


Fig. 3: Mean transmitted power versus antenna spacing (d_x) at $K = 1$, $K = 2$, and $K = 4$.

power. For $K = 1$, FD and OP2-UW achieve nearly the same mean transmit power (4.62 dBm), indicating that the proposed optimization algorithm for DMA performs robustly. Algorithm 1 for solving (11) yields the same result as the optimal solution of (11) when the DoF for both problems are the same. However, as K increases to 2 and beyond, FD begins to outperform OP2-UW, benefiting from a larger number of optimization variables.

Finally, in Fig. 3, we present the results analyzing the effect of antenna spacing d_x in DMA to achieve the same performance as conventional FD-based architectures with $d_x = \lambda/2$. Simulations were conducted with a minimum rate constraint $R_{\min,k} = 20$ bits/s/Hz, separately for different numbers of users $K = 1$, $K = 2$, and $K = 4$, and for various antenna spacings d_x of the DMA. For a fair comparison, the aperture size was kept constant, where smaller values of d_x resulted in a higher number of antennas $N_c = \lfloor D/d_x \rfloor$. As expected, the results in Fig. 3 demonstrate that as the antenna spacing d_x decreases, the performance of the DMA gradually improves, and the performance gap relative to FD with $d_x = \lambda/2$ narrows. Numerically, for $K = 1$, DMA surpasses FD performance at $d_x = \lambda/4$, and for $K = 2$, at nearly $d_x = \lambda/4$. For $K = 4$, the performance gap relative to FD decreases as d_x reduces, from 8.9 dB at $d_x = \lambda$ to 2.3 dB at $d_x = \lambda/4$, with DMA outperforming FD beyond $d_x = \lambda/6$. It is important to note that DMA offers additional efficiency gains due to lower power consumption from its reduced number of RF chains, although this aspect is not considered in this analysis. Specifically, DMA requires significantly fewer RF chains, with $N_r = 18$ for $d_y = \lambda/2$, compared to FD with $N = N_r \times N_c = 818$ for $d_x = \lambda/2$ and $d_y = \lambda/2$. These results suggest that when using DMA for beamforming applications, element spacing should be carefully selected based on the number of users.

V. CONCLUSION

In this work, we investigated DMA-aided multi-user MISO systems under minimum achievable rate constraints with the

joint optimization of DMA weights and digital precoders, aiming to minimize transmitted power. We demonstrated that the joint optimization for DMA yields the same result with FD when the DoF for both scenarios are the same, i.e., specifically in the case of $K = 1$ and without any Lorentzian constraints on DMA weights. For higher number of users and simulation with Lorentzian constraints of DMA weights, the performance gap is presented caused by reduced DoF for DMA. Moreover, impact of Lorentzian constraints on this gap is shown to slightly increase as the number of users within the network increases, whereas this gap remains constant for higher requirement of achievable rate in the same setup. On the other hand, impact of the reduction in the number of optimization variables has more significant impact, leading to a more dramatic increase in the performance gap with the increase of number of users. It has also been shown that, as the number of users increases, a denser antenna placement is required for DMA to outperform FD with a reduced number of RF chains. Considering these insights, the impact of RF chains on power efficiency and the exploration of DoF for systems with a massive number of devices in DMA-aided configurations could be potential topics for future research.

ACKNOWLEDGMENT

This work was supported by UK Research and Innovation under the UK government's Horizon Europe funding guarantee through MSCA-DN SCION Project Grant Agreement No.101072375 [Grant Number: EP/X027201/1].

REFERENCES

- [1] C.-X. Wang, X. You, X. Gao, X. Zhu, Z. Li, C. Zhang, H. Wang, Y. Huang, Y. Chen, H. Haas, J. S. Thompson, E. G. Larsson, M. Di Renzo, W. Tong, P. Zhu, X. Shen, H. V. Poor, and L. Hanzo, "On the road to 6G: Visions, requirements, key technologies, and testbeds," *IEEE Commun. Surv. Tutor.*, vol. 25, no. 2, pp. 905–974, 2023.
- [2] T. Huang, W. Yang, J. Wu, J. Ma, X. Zhang, and D. Zhang, "A survey on green 6G network: Architecture and technologies," *IEEE Access*, vol. 7, pp. 175 758–175 768, 2019.
- [3] N. Shlezinger, G. C. Alexandropoulos, M. F. Imani, Y. C. Eldar, and D. R. Smith, "Dynamic metasurface antennas for 6G extreme massive MIMO communications," *IEEE Wireless Commun.*, vol. 28, no. 2, pp. 106–113, 2021.
- [4] H. Zhang, N. Shlezinger, F. Guidi, D. Dardari, M. F. Imani, and Y. C. Eldar, "Beam focusing for near-field multiuser MIMO communications," *IEEE Trans. Commun.*, vol. 21, no. 9, pp. 7476–7490, 2022.
- [5] A. Azarbahram, O. L. A. López, R. D. Souza, R. Zhang, and M. Latva-Aho, "Energy beamforming for RF wireless power transfer with dynamic metasurface antennas," *IEEE Wireless Commun. Lett.*, vol. 13, no. 3, p. 781–785, 2024.
- [6] N. Shlezinger, O. Dicker, Y. C. Eldar, I. Yoo, M. F. Imani, and D. R. Smith, "Dynamic metasurface antennas for uplink massive MIMO systems," *IEEE Trans. Commun.*, vol. 67, no. 10, pp. 6829–6843, 2019.
- [7] S. W. Ellingson, "Path loss in reconfigurable intelligent surface-enabled channels," in *2021 IEEE 32nd Annual International Symposium on Personal, Indoor and Mobile Radio Communications (PIMRC)*, Helsinki, Finland, Sep 2021, pp. 829–835.
- [8] M. Bengtsson and B. Ottersten, "Optimal and suboptimal transmit beamforming," in *Handbook of Antennas in Wireless Communications*, L. C. Godara, Ed. Boca Raton, FL: CRC Press, 2001.
- [9] M. Grant and S. Boyd, "CVX: Matlab software for disciplined convex programming, version 2.1," <https://cvxr.com/cvx>, 2014.